Structural, Magnetic, and Optical Studies of New Mixed-valence Copper(II)–Platinum(IV) Complexes with One-dimensional Chain Structures†

Hiroki Oshio,* Koshiro Toriumi, and Shunji Bandow
Applied Molecular Science, Institute for Molecular Science, Okazaki National Research Institutes, Myodaiji, Okazaki 444, Japan
Kensuke Miyagawa and Susumu Kurita
Laboratory of Applied Physics, Faculty of Engineering, Yokohama National University, Hodogaya, Yokohama 240, Japan

The crystal structures of halogen-bridged one-dimensional copper(II)–platinum(IV) complexes $[Cu(en)_2][PtX_2(en)_2][ClO_4]_4$ (en = ethylenediamine, X = Cl or Br) have been determined by *X*-ray structure analyses. The chloro-bridged complex (**1**) crystallizes in the orthorhombic space group *Icma* with unit-cell dimensions *a* = 13.645(1), *b* = 10.787(1), *c* = 9.645(1) Å, and *Z* = 2. The bromo-bridged complex crystallizes as two different non-stoicheiometric compounds (**2a**) and (**2b**) depending on the preparation conditions. Both compounds crystallize in the orthorhombic space group *Icma* with *a* = 13.599(1), *b* = 10.917(1), *c* = 9.657(1) Å, and *Z* = 2 for (**2a**) and *a* = 13.625(2), *b* = 10.905(2), *c* = 9.651(1) Å, and *Z* = 2 for (**2b**). In (**1**), (**2a**), and (**2b**), the copper(II) and platinum(IV) complexes which are bridged by a halogen atom are stacked alternately, leading to a one-dimensional chain structure. The *X*-ray structure analyses using a full-matrix least-squares method revealed the non-stoicheiometric structures, in which the Cu^{II} and Pt^{IV} are partially replaced by Pt^{II}. The temperature dependence of the magnetic susceptibilities and e.s.r. measurements show no strong magnetic interaction between the copper atoms. Single-crystal reflectance spectra of complex (**1**) show a polarized band (parallel to the chain direction) at 2.7—2.8 eV corresponding to $Cu^{II} \longrightarrow Pt^{IV}$ charge transfer. A progression of peaks (313, 625, and 940 cm^{-1}) due to the totally symmetric stretching mode of Cl–Pt^{IV}–Cl was observed in the resonance-Raman spectrum of complex (**1**).

One-dimensional halogen-bridged M^{II}–M^{IV} mixed-valence complexes (M = Pt, Pd, or Ni), which are analogous to the so-called Wolffram's red salt, have been extensively studied,[1–4] because they have an extremely strong electron–lattice coupling within the chain structure. This type of system consists of either a pair of complexes having the same metal ions with different oxidation states or a combination of two kinds of complexes having different diamagnetic platinum group metal ions in each oxidation state.[5–8] It is well known that charge-transfer properties between two metal ions or molecules can be used to design a molecular ferromagnet or highly electric conducting material.[9,10] If paramagnetic heterometal ions can be introduced into such chain systems a study of the charge-transfer properties between heterometal ions can be made. It is also expected that a higher electrical conductivity or some interesting magnetic and optical behaviours may result, if appropriate metal ions are chosen. Here the syntheses, molecular structures, magnetic and spectroscopic properties of new one-dimensional halogen-bridged heterometal complexes are reported. A part of this work was preliminarily reported.[11]

Experimental

Crystal Growth of $[Cu(en)_2][PtCl_2(en)_2][ClO_4]_4$ (**1**) (*en = ethylenediamine*).—Red needle crystals were grown by slow evaporation of an aqueous solution (5 cm^3) containing $[PtCl_2(en)_2]Cl_2$ (1 mmol), $[Cu(en)_2]Cl_2$ (1 mmol), and $NaClO_4$ (4 mmol) (Found: C, 10.20; H, 3.35; Cu, 6.00; N, 11.85. Calc. for $C_8H_{32}Cl_6Cu_{0.89}N_8O_{16}Pt_{1.11}$: C, 9.80; H, 3.30; Cu, 5.75; N, 11.40%).

$[Cu(en)_2][PtBr_2(en)_2][ClO_4]_4$ (**2a**) *and* (**2b**).—The procedure outlined above was used. When the solution was evaporated slowly, complex (**2a**) was obtained (Found: C, 9.00; H, 3.10; Cu, 3.50; N, 10.55. Calc. for $C_8H_{32}Br_{1.70}Cl_4Cu_{0.56}N_8O_{16}Pt_{1.44}$: C, 8.80; H, 2.95; Cu, 3.25; N, 10.30%). The solution was concentrated to 2 cm^3 on a hot plate and allowed to stand for 3 h in a refrigerator, when complex (**2b**) was obtained (Found: C, 9.20; H, 3.20; Cu, 3.95; N, 10.70. Calc. for $C_8H_{32}Br_{1.55}Cl_4Cu_{0.64}N_8O_{16}Pt_{1.36}$: C, 9.00; H, 3.00; Cu, 3.80; N, 10.50%).

Physical Measurements.—E.s.r. spectra. Single-crystal e.s.r. spectra were recorded at 10 K on a JEOL FE2XG spectrometer (field modulation 100 kHz) equipped with a low-temperature cell (Air Products LTD-3-110). Aligned crystals, of which the chain axes (*b* axes) are parallel to each other, were used to measure the parallel and perpendicular components.

Reflectance spectra. The reflectance spectra were measured on the flat plate surface of an as-grown single crystal. The sample was immersed directly in liquid nitrogen. The light beam, whose angle of convergence was $\pm 3.3\%$, was directed normal to the surface of the crystal. The reflected light was detected with photomultipliers (HAMAMATSU R928, R406).

Raman spectra. The Raman spectra of single crystals at 77 K were measured in the backward scattering configuration with the incident light directed normal to the surface of the specimens. Excitation at 514.5 nm was with a NEC argon-ion laser. The Raman spectrum was recorded on monochromator equipped with a HAMAMATSU digital photometer system.

Magnetic susceptibility. The magnetic susceptibility of

Supplementary data available: see Instructions for Authors, *J. Chem. Soc., Dalton Trans.*, 1990, Issue 1, pp. xix—xxii.
Non-S.I. unit employed: eV $\approx 1.60 \times 10^{-19}$ J.

Table 1. Data collection and processing parameters[a] for $[Cu(en)_2][PtCl_2(en)][ClO_4]_4$ (**1**) and $[Cu(en)_2][PtBr_2(en)_2][ClO_4]_4$ (**2a**) and (**2b**)

Compound	(1)	(2a)	(2b)
Formula	$C_8H_{32}Cl_6CuN_8O_{16}Pt$	$C_8H_{32}Br_2Cl_4CuN_8O_{16}Pt$	
M	967.73	1 056.63	1 056.63
a/Å	13.645(1)	13.599(1)	13.625(2)
b/Å	10.787(1)	10.917(1)	10.905(2)
c/Å	9.645(1)	9.657(1)	9.651(1)
U/Å^3	1 419.6(2)	1 433.6(2)	1 433.9(4)
D_c[b]/g cm^{-3}	2.297	2.526	2.473
μ(Mo-K_α)/cm^{-1}	65.99	93.50	93.50
Sample size/mm	0.30 × 0.08 × 0.08	0.27 × 0.08 × 0.08	0.32 × 0.07 × 0.07
Scan speed (ω)/° min^{-1}	4	3	4
Total data collected	2 815	2 859	2 311
Independent data [$F_o > 3\sigma(F_o)$]	991	884	751
Total variables	83	84	84
R[c]	0.025	0.022	0.041
R'[d]	0.039	0.025	0.049
Weighting function	$[\sigma_c^2 + (0.02\|F\|)^2]^{-1}$	$[\sigma_c^2 + (0.015\|F\|)^2]^{-1}$	$[\sigma_c^2 + (0.02\|F\|)^2]^{-1}$

[a] Details in common: Mo-K_α radiation, λ = 0.710 73 Å; orthorhombic; space group *Icma*; Z = 2; colour, red; Rigatu AFC5 diffractometer; 2θ range, 2—65°; octant $-20 < h < 20, 0 < k < 16, 0 < l < 14$; scan width, 1.3 + 0.5 tan θ; maximum scan time, 2 s; scan method, ω—2θ. [b] Non-stoicheiometry of the crystal was considered in the density calculation. [c] $R = \Sigma(|F_o| - |F_c|)/\Sigma|F_o|$. [d] $R' = (|F_o| - |F_c|)^2/\Sigma w|F_o|^2]^{\frac{1}{2}}$, $w = 1/\sigma^2(|F_o|)$.

Table 2. Positional parameters (× 10^4) and occupancy factors with their estimated standard deviations (e.s.d.s) for $[Cu(en)_2][PtCl_2(en)_2][ClO_4]_4$ (**1**)

Atom	x	y	z	Occupancy
Pt	0	2 500	0	0.555(5)
Cu	0	2 500	0	0.455
Cl(1)	0	4 644(3)	0	0.5
Cl(2)	2 978(1)	5 000	790(2)	
N	994(3)	2 460(4)	1 566(4)	
C	493(5)	2 812(5)	2 876(5)	
O(1)	2 635(5)	3 911(4)	178(5)	
O(2)	4 041(10)	5 000	257(17)	0.5
O(3)	3 097(21)	5 000	2 181(13)	0.5
O(2')	3 821(14)	5 000	1 497(43)	0.5
O(3')	2 180(18)	5 000	1 928(16)	0.5

powdered samples was measured by an Oxford Faraday-type magnetic balance system equipped with a superconducting magnet. Temperature readings were calibrated with a magnetic thermometer by the use of $[Cr(NH_3)_3Cl_3]$.

X-Ray Structure Determinations.—Details of data collection and refinements are given in Table 1. The structures were solved by a heavy-atom method and refined by full-matrix least squares with anisotropic thermal parameters for non-H atoms and isotropic for H atoms. Occupancy factors of the metal ions in complex (**1**) and both metal and bridging bromide ions in (**2a**) and (**2b**) were included in the refinements. Atomic scattering factors and anomalous scattering corrections were taken from ref. 12. Final atomic parameters for non-hydrogen atoms are listed in Tables 2 and 3. Oscillation and Weissenberg photographs were carefully taken for the single crystals. All the calculations were carried out on a HITAC M680 computer at the Computer Center of the Institute of Molecular Science with the Universal Crystallographic Computation Program System UNICS III.[13]

Additional material available from the Cambridge Crystallographic Data Centre comprises H-atom co-ordinates, thermal parameters, and remaining bond lengths and angles.

Results and Discussion

Description of the Structures.—Crystals of complexes (**1**), (**2a**), and (**2b**) contain $[Cu(en)_2]^{2+}$, $[PtX_2(en)_2]^{2+}$ (X = Cl or Br), and ClO_4^-. The copper and platinum complexes which are bridged by halogen atoms have linear chain structures. These crystals are isomorphous with the halogen-bridged M^{II}–M^{IV} mixed-valence compounds $[M(en)_2][MX_2(en)_2][ClO_4]_4$ (M = Pt or Pd, X = Cl or Br).[14,15] Selected interatomic distances, angles, and hydrogen-bond distances for the three complexes and an ORTEP diagram of (**1**) are shown in Table 4 and Figure 1, respectively.

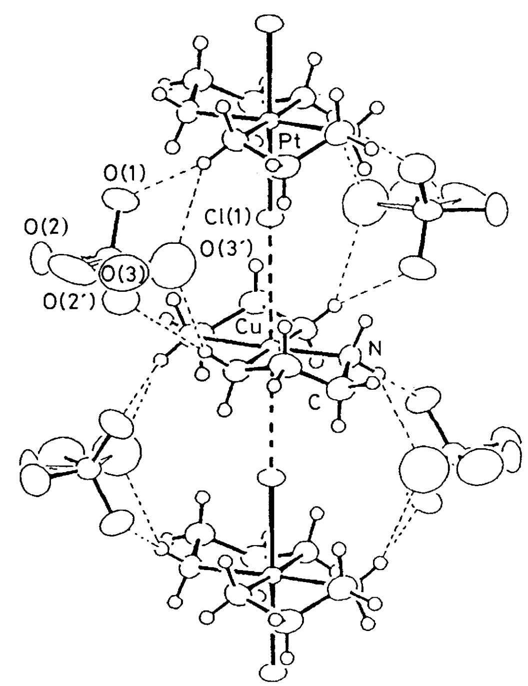

Figure 1. ORTEP diagram of $[Cu(en)_2][PtCl_2(en)_2][ClO_4]_4$ with 50% probability. The broken lines correspond to the hydrogen bonds. The perchlorate ion is disordered at two orientations on a mirror plane

The platinum and copper atoms are co-ordinated by two ethylenediamines and the metal–nitrogen distances are 2.031(4), 2.043(3), and 2.043(6) Å for complexes (**1**), (**2a**), and (**2b**), respectively. The octahedral six-co-ordinate $Pt^{IV}X_2(en)_2$ and the square-planar four-co-ordinate $Cu^{II}(en)_2$ units are arranged alternately, in a linear chain structure along the b axis. As for

Table 3. Positional parameters (× 10^4) and occupancy factors with their e.s.d.s for $[Cu(en)_2][PtBr_2(en)_2][ClO_4]_4$ (**2a**) and (**2b**)

	Complex (**2a**)				Complex (**2b**)			
Atom	*x*	*y*	*z*	Occupancy	*x*	*y*	*z*	Occupancy
Pt	0	2 500	0	0.72(4)	0	2 500	0	0.68(1)
Cu	0	2 500	0	0.28	0	2 500	0	0.32
Br	0	4 747(1)	0	0.43(5)	0	4 734(2)	0	0.39(5)
Cl	2 987(1)	5 000	790(2)		2 987(3)	5 000	775(4)	
N	1 001(3)	2 470(5)	1 578(4)		1 000(4)	2 470(8)	1 576(7)	
C	497(4)	2 795(4)	2 890(5)		508(8)	2 831(9)	2 874(9)	
O(1)	2 631(4)	3 928(3)	190(5)		2 631(7)	3 929(6)	187(10)	
O(2)	4 057(11)	5 000	290(14)	0.5	4 029(19)	5 000	278(26)	0.5
O(3)	3 053(22)	5 000	2 205(15)	0.5	3 022(41)	5 000	2 170(26)	0.5
O(2′)	3 846(12)	5 000	1 436(36)	0.5	3 861(25)	5 000	1 422(68)	0.5
O(3′)	2 254(16)	5 000	1 916(19)	0.5	2 221(30)	5 000	1 885(41)	0.5

Table 4. Interatomic distances (Å), angles (°), and hydrogen-bond distances (Å) of $[Cu(en)_2][PtX_2(en)_2][ClO_4]_4$ [X = Cl for (**1**), Br for (**2a**) and (**2b**)], and bond-length ratios

	(**1**)	(**2a**)	(**2b**)
M*–X	2.313(3)	2.453(1)	2.436(2)
M–X	3.081(3)	3.005(1)	3.016(2)
M–N	2.031(4)	2.043(3)	2.043(6)
N–C	1.486(6)	1.483(6)	1.475(11)
C–C^{I}	1.505(12)	1.497(11)	1.561(22)
Cl(2)–O(1)	1.395(5)	1.393(4)	1.387(8)
Cl(2)–O(2)	1.540(14)	1.533(14)	1.498(27)
Cl(2)–O(3)	1.351(13)	1.369(15)	1.347(26)
Cl(2)–O(2′)	1.337(26)	1.325(22)	1.344(43)
Cl(2)–O(3′)	1.546(21)	1.475(20)	1.496(40)
M–N–C	108.6(3)	109.0(3)	109.0(5)
X–M–N	91.2(1)	90.9(1)	90.9(2)
N–C–C^{I}	107.3(4)	108.3(4)	106.3(8)
O(1)–Cl(2)–O(2)	100.0(6)	101.5(6)	101.6(11)
O(1)–Cl(2)–O(3)	117.4(6)	116.0(6)	114.9(11)
O(1)–Cl(2)–O(2′)	120.3(12)	120.2(10)	120.0(19)
O(1)–Cl(2)–O(3′)	93.7(8)	94.1(8)	92.8(16)
O(2)–Cl(2)–O(3)	102.6(8)	104.6(8)	106.7(15)
O(2′)–Cl(2)–O(3′)	104.1(14)	104.3(12)	106.6(24)
Pt–X/Cu–X	0.751	0.816	0.808
NH ··· O(1)	3.043(7)	3.040(6)	3.044(12)
NH ··· O(1^{II})	3.167(7)	3.187(6)	3.187(12)
NH ··· O(3)	3.201(13)	3.261(13)	3.235(23)

* M denotes the metal ion. Shorter and longer bond lengths were considered to be Pt–X and Cu–X, respectively. Key to symmetry operations: (I) $-x, \frac{1}{2} - y, z$; (II) $x, \frac{1}{2} - y, -z$.

the analogous M^{II}–M^{IV} mixed-valence compounds, the bridging halogen atom is positionally disordered at two sites related by a two-fold axis equidistant from the midpoint between two metal sites with an occupancy factor of 0.5. The Cu^{II} and Pt^{IV} atoms are also disordered at a metal site, and cannot be distinguished from each other in the crystal. The alternation of $[PtX_2(en)_2]^{2+}$ and $[Cu(en)_2]^{2+}$ complexes in the linear chain is, however, confirmed by the diffuse scattering with plane shapes (indexed to $k + \frac{1}{2}$) observed in the *X*-ray photographs of (**1**), (**2a**), and (**2b**). The perchlorate ions are located on a mirror plane equidistant between two metal ions. Two oxygen atoms of the perchlorate ion are positionally disordered at two sites respectively on a mirror plane, showing orientational disorder of the ion. The perchlorate ions, which have the same geometry as in the Pt^{II}–Pt^{IV} system,[14,15] participate in hydrogen bonds with NH groups of the ethylenediamine ligand, ranging from 3.040(6) to 3.261(13) Å. These hydrogen bonds support the chain structure.

Results of full-matrix least-squares calculations in which occupancy factors at the metal site for complex (**1**), and both the metal and halogen-bridged sites for (**2a**) and (**2b**), were included in the refinements show non-stoicheiometric structures (Tables 2 and 3). These structures can be interpreted by a partial substitution of the copper(II) complex by the platinum(II) complex during preparation. In (**2a**) and (**2b**) the deficiency of the bridging bromide ion may suggest that the platinum(IV) unit was partially substituted by the copper(II) or platinum(II) units. It is noted that the rapid evaporation of the solution containing $[PtBr_2(en)_2]Br_2$, $[Cu_2(en)_2]Br_2$, and $NaClO_4$ tends to give compounds whose copper contents are lower than the stoicheiometric value.

In a similar manner to the structure determination of Wolffram's red salt,[14,15] it can be considered that the shorter metal to halogen distances correspond to the Pt^{IV}–X distance, the longer ones to the Cu^{II} ··· X distances. The interatomic distances between copper and bridging halogen atoms are extremely long compared with a macrocyclic tetra-aminecopper(II) complex in which the apical Cu-Cl distance is 2.716(11) Å.[16,17] The weak interaction between copper and bridging halogen atoms may cause a blue shift of the *d–d* transition which results in the red colour of the crystal. It is also expected that the charge-transfer band between the copper and platinum ions may result in the red colour. It is interesting that the bond distances between metals and bridging halogen atoms in the Cu^{II}–Pt^{IV} systems [Pt–Cl 2.313(3), Cu ··· Cl 3.081(3) Å for (**1**) and Pt–Br 2.436(2), Cu ··· Br 3.016(2) Å for (**2b**)] are similar to the corresponding values in $[Pt^{II}(en)_2][Pt^{IV}X_2(en)_2][ClO_4]_4$, that is 2.318 and 3.085 Å for the chloro-bridged complex and 2.473 and 2.997 Å for the bromo-bridged complex. Comparing the metal–bromine distances of (**2a**) and (**2b**), the distances become closer to those of $[Pt^{II}(en)_2][Pt^{IV}Br_2(en)_2][ClO_4]_4$ as the copper population decreases. The bond-distance ratios of M^{IV}–X to M^{II}–X are considered to be related to the electronic interaction between two metal atoms. That is, the closer the values to unity the stronger interaction between the metal ions. For example, in the series $[Pt^{II}(en)_2][Pt^{IV}X_2(en)_2][ClO_4]_4$ (X = Cl, Br, or I) the ratio for the iodo-bridged complex, which shows the strongest electronic interaction, is the largest (0.919).[14] It should be noted that the ratios for the Cu–X–Pt system [0.751, 0.816, and 0.808 for (**1**), (**2a**), and (**2b**), respectively] are close to those for the $[Pt^{II}(en)_2][Pt^{IV}X_2(en)_2][ClO_4]_4$ system (0.751 and 0.825 for X = Cl and Br, respectively).[14]

The successful syntheses of the series $[Cu^{II}(en)_2][Pt^{IV}X_2(en)_2][ClO_4]_4$ seems to be due to the elongated octahedral structure of the copper(II) ethylenediamine complex due to the Jahn–Teller distortion. That is, the similarity of the stereochemistry of copper(II) and platinum(II) ethylenediamine complexes makes the chain formation possible. We also tried to

Table 5. E.s.r. and magnetic parameters of $[Cu(en)_2][PtX_2(en)_2][ClO_4]_4$ [X = Cl for (**1**), Br for (**2a**) and (**2b**)]

	(**1**)	(**2a**)	(**2b**)
$g_{\parallel}$	2.048	2.044	2.044
$g_{\perp}$	2.167	2.167	2.167
Curie constant (e.m. units K mol^{-1})	0.415	0.495	0.486
Weiss constant (*K*)	−1.2	−3.22	−1.67

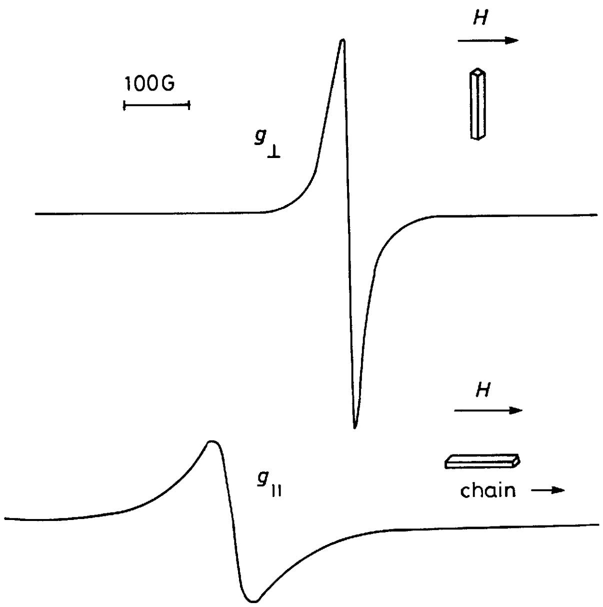

Figure 2. Single-crystal e.s.r. spectra of $[Cu(en)_2][PtCl_2(en)_2][ClO_4]_4$ measured at 10 K

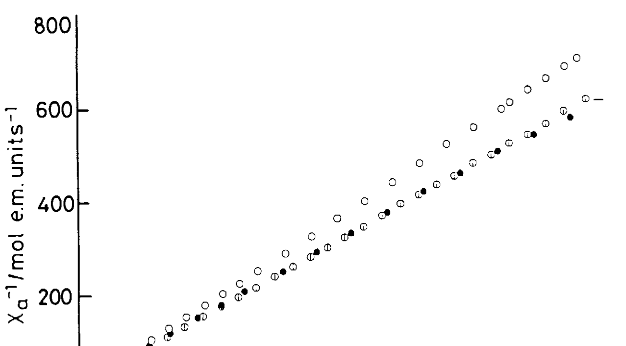

Figure 3. Magnetic susceptibility data for $[Cu(en)_2][PtCl_2(en)_2][ClO_4]_4$ (**1**) (○) and $[Cu(en)_2][PtBr_2(en)_2][ClO_4]_4$ (**2a**) (●) and (**2b**) (◐)

synthesize an iodo-bridged complex, however in vain because $[Pt^{IV}I_2(en)_2]^{2+}$ was easily reduced to $[Pt^{II}(en)_2]^{2+}$ which formed the more stable $[Pt^{II}(en)_2][Pt^{IV}I_2(en)_2][ClO_4]_4$.

Magnetic Properties.—Single-crystal e.s.r. spectra for complex (**1**) at 10 K are shown in Figure 2 and the anisotropic g values are listed in Table 5. No hyperfine splitting was resolved. The spectra show the typical pattern for an octahedral copper(II) complex with Jahn–Teller distortion. Applying a magnetic field perpendicular to the chain direction (b axis), the perpendicular component of the g tensor was obtained, while on applying a magnetic field parallel to the chain direction the parallel component was obtained. According to the spectra, the electron spin on the copper atom resides in the $d_{x^2-y^2}$ orbital which is perpendicular to the chain direction (b axis). The temperature dependence of the magnetic susceptibility for the complexes was also measured from 270 K down to liquid-helium temperature. The susceptibilities obey the Curie–Weiss law (Figure 3) and estimated Curie and Weiss constants are listed in Table 5. The negative values of the Weiss constants are due to the weak antiferromagnetic interaction between paramagnetic copper ions. The facts that the direction of the magnetic orbital ($d_{x^2-y^2}$) of the copper atom is perpendicular to the chain direction and the d_{z^2} orbital of platinum(IV) is vacant might be responsible for the weak magnetic interaction.

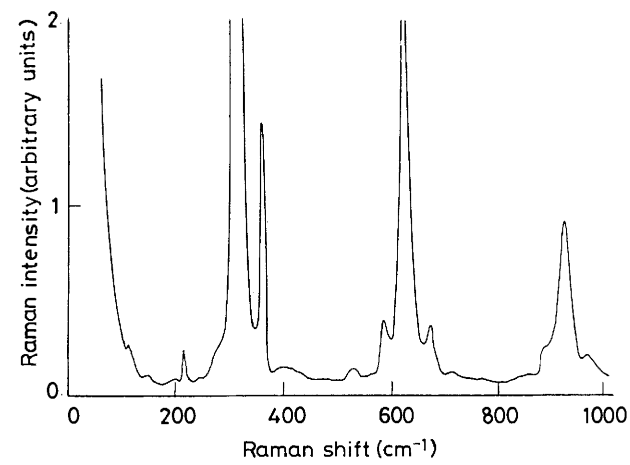

Figure 4. Resonance-Raman spectrum of $[Cu(en)_2][PtCl_2(en)_2][ClO_4]_4$ single crystal at 77 K with 514.5 nm excitation. Both incident and scattered light are polarized parallel to the chain axis.

Raman Spectrum.—The resonance Raman spectrum of compound (**1**), at 77 K using excitation by an argon ion laser at 514.5 nm, is shown in Figure 4 where both the incident and scattered light were polarized parallel to the chain. The spectrum is dominated by an intense progression (313, 625, and 940 cm^{-1}) of the totally symmetric Cl–Pt^{IV}–Cl stretching mode. The intensity enhancement relies on the charge-transfer excitation (Cu^{II}–Pt^{IV}) by the laser light. A strong band corresponding to the asymmetric stretching mode of Cl–Pt^{IV}–Cl also appeared at 360 cm^{-1}. Though this band is Raman inactive, imperfect properties such as structural defects due to non-stoicheiometry make it observable. It is interesting that the wavenumbers (313 and 360 cm^{-1}) for the totally symmetric and asymmetric stretching modes are respectively similar to the values for $[Pt(en)_2][PtCl_2(en)_2][ClO_4]_4$ (310 and 359 cm^{-1}).[18]

U.V.–Visible Spectra.—Single-crystal reflectance and absorption spectra of $[Cu(en)_2][PtCl_2(en)_2][ClO_4]_4$ measured at 77 K are depicted in Figure 5. As the absorption spectra were obtained by a transmission method, a strong absorption band around 2.75 eV which is deduced from the reflectance spectrum shows a saturation in intensity. This strong band, which appears at 2.7—2.8 eV in the reflectance spectrum and starts to grow at 2.35 eV in the absorption spectrum, can be assigned to a charge-transfer band from Cu^{II} to Pt^{IV}, because it is strongly polarized along the b axis (chain direction) and is not observed for an aqueous solution of the compound. It should also be noted that in the Raman spectrum the totally symmetric stretching mode due to Cl–Pt^{IV}–Cl was resonance-enhanced when this charge-transfer band (514.5 nm) was excited. When

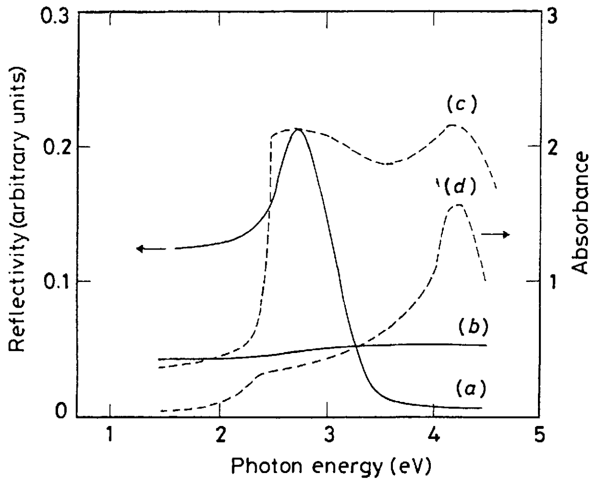

Figure 5. U.v.–visible spectra of $[Cu(en)_2][PtCl_2(en)_2][ClO_4]_4$ as a single crystal at 77 K. Reflectance spectra (solid line) and absorption spectral (broken line) [(*a*), (*c*) parallel; (*b*), (*d*) perpendicular to the *b* axis]. As the absorption spectra were measured by a transmission method, a strong band at 2.7—2.8 eV shows saturation in the absorption spectrum (*c*)

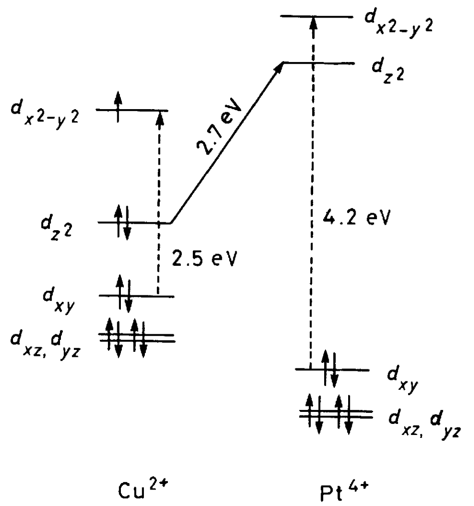

Figure 6. Energy diagram and spectral assignment of $[Cu(en)_2][PtCl_2(en)_2][ClO_4]_4$ (**1**)

the electric vector of the incident light was perpendicular to the *b* axis, weak bands at 2.5 and 4.2 eV were observed and were assigned to the *d–d* band ($d_{xy} \longrightarrow d_{x^2-y^2}$) of Cu^{II} and Pt^{IV}, respectively (see Figure 6). It is surprising that the charge-transfer band of this system appears in a very similar region to that (2.72 eV) of the Pt^{II}–Pt^{IV} system[7] and this experimental result implies that the energy level of the Cu^{2+} d_{z^2} orbital is accidentally coincident with that of the Pt^{2+} ion.

Conclusion

New heterometal mixed-valence compounds $[Cu^{II}(en)_2][Pt^{IV}X_2(en)_2][ClO_4]_4$ (X = Cl or Br) were prepared and crystal-structure analyses revealed halogen-bridged one-dimensional chain structures in which the copper and platinum complexes are arranged alternately. The resonance-Raman spectrum using excitation at 514.5 nm shows the progression of the totally symmetric Cl–Pt^{IV}–Cl stretching. Optical spectra show a strong band at 2.7 eV which is assigned to the charge-transfer band from Cu^{II} to Pt^{IV}. E.s.r. and magnetic susceptibility studies show the absence of strong magnetic interactions between the paramagnetic copper(II) centres. It is suggested that a paramagnetic metal ion, which has an electron spin in a d_{z^2} orbital, should be introduced into the chain system in order to achieve strong magnetic interactions between the metal ions through the bridging halogen atoms.

References

1 R. J. H. Clark, V. B. Croud, and M. Kurmoo, *J. Chem. Soc., Dalton Trans.*, 1985, 815.
2 R. J. H. Clark, V. B. Croud, and A. R. Kholhar, *Inorg. Chem.*, 1987, **26**, 3284.
3 H. Toftlund and O. Simonsen, *Inorg. Chem.*, 1984, **23**, 4261.
4 K. Toriumi, Y. Wada, T. Mitani, S. Bandow, M. Yamashita, and Y. Fujii, *J. Am. Chem. Soc.*, 1989, **111**, 2341.
5 R. J. H. Clark and V. B. Croud, *Inorg. Chem.*, 1986, **25**, 1751.
6 K. Toriumi, M. Yamashita, and I. Murase, *Chem. Lett.*, 1986, 1753.
7 Y. Wada, T. Mitani, K. Toriumi, and M. Yamashita, *J. Phys. Soc. Jpn.*, 1985, **54**, 3143.
8 R. J. H. Clark, V. B. Croud, R. J. Wills, P. A. Bates, H. M. Dawes, and M. B. Hursthouse, *Acta Crystallogr., Sect. B*, 1989, **45**, 147.
9 T. J. LePage and R. Breslow, *J. Am. Chem. Soc.*, 1987, **109**, 6412.
10 J. S. Miller, J. C. Calabrese, H. Rommelmann, S. R. Chitipeddim, J. H. Zhang, W. Reiff, and A. J. Epstein, *J. Am. Chem. Soc.*, 1987, **109**, 769.
11 H. Oshio, K. Toriumi, and S. Bandow, *Chem. Lett.*, 1988, 1713.
12 'International Tables for *X*-Ray Crystallography,' Kynoch Press, Birmingham, 1974, vol. 4.
13 T. Sakurai and K. Kobayashi, *Rigaku Kenkyusho Hokoku*, 1979, **55**, 69.
14 N. Matsumoto, M. Yamashita, and S. Kida, *Bull. Chem. Soc. Jpn.*, 1978, **51**, 2334.
15 M. Yamashita, K. Toriumi, and T. Ito, *Acta Crystallogr., Sect. C*, 1985, **41**, 876.
16 T. J. Lee, T. Y. Lee, W. B. Juang, and C. S. Chung, *Acta Crystallogr., Sect. C*, 1985, **41**, 1745.
17 L. Sato, T. Legros, M. Molla, and J. Garcia, *Acta Crystallogr., Sect. C*, 1987, **43**, 834.
18 S. D. Allen, R. J. H. Clark, V. B. Croud, and M. Kurmoo, *Philos. Trans. R. Soc. London, Ser. A*, 1985, **314**, 131.

Received 22*nd May* 1989; *Paper* 9/02130B